GEO-SEQ Quarterly Report: October 1, 2005 to December 31, 2005

Earth Sciences Division
Lawrence Berkeley National Laboratory
Berkeley, California 94720

Contact: Dr. Sally M. Benson
Earth Sciences Division
Lawrence Berkeley National Laboratory
1 Cyclotron Rd., MS 90-1116
510-486-5875; smbenson@lbl.gov

DOE Program Manager: Karen Cohen, 412-386-6667

Highlights

- Mapping migration of CO_2 using X-well seismic and Vertical Seismic Profiling (VSP) in a saline formation has been demonstrated for the first time at the Frio Brine Pilot.
- A new method for measuring field-scale relative permeability from pressure transient test data has been developed.
- Five papers describing the Frio Brine Pilot were presented at the AGU Annual Meeting in December 2005. This completes the FY06 QTR1 Milestone.
- Planning for Phase II of the Frio Brine Formation Pilot Tests has begun.
- Collaboration between LBNL and CO2CRC for the Otway project has begun. Several meetings and discussion have taken place in order to define current workscopes between groups.

Project Milestones

Task	Deliverable Date

QTR 1
Submit abstract to the Fall 2005 AGU meeting on Frio Formation CO_2 Injection Studies.
  • Five abstracts were submitted and accepted for presentations and posters.
  • Abstracts are attached to this report.
	December 30, 2005 - Complete

QTR 2 Design of geophysical monitoring and fluid sampling for Frio II.	March 30, 2006
QTR 3 Submit abstract(s) to the 5th Annual National Carbon Sequestration Conference held in May, 2006 in Alexandria,Virginia.	June 30, 2006
QTR 4 Initiate data collection for the Frio II Pilot Test.	September 30, 2006

Research Progress Report

Task 1. Phase II for the Frio Brine Formation Pilot Tests.

To prepare for the Frio II Pilot test, detailed simulations of CO_2 transport will be carried out based on the results obtained from the Frio Brine Pilot Test conducted in FY2004. This work will take advantage of new insights on multiphase flow, solubility trapping and mineral trapping that were gained from the short-term pilot test conducted during FY2004. The numerical simulators TOUGH2 and TOUGHREACT will be used for these studies.

More reliable estimates for the amount of CO_2 that can be stored per unit volume of the Frio Formation will be developed based on what we now know about field-scale relative permeability and CO_2 pore volume occupancy. Field-derived values for these parameters will be used as input to the TOUGH2 simulator and combined with realistic geology to perform numerical simulations of CO_2 storage capacity for the Frio. As a second part of the planning study, the amount of CO_2 that can be stored by solubility and mineral trapping will be assessed using TOUGHREACT. Again, improved understanding and estimates will be based on geochemical data obtained from the Frio Brine Pilot I. Specifically, we will use mineralogical data obtained from cores collected during drilling the new injection well at the test site and water samples collected during the CO_2 injection, which provided new data on CO_2, brine and formation interactions.

Field testing for Phase II of the CO_2 injection test at the Frio Test Site will be carried out in cooperation with the Texas Bureau of Economic Geology. The goals of the experiment are designed to answer extremely important questions not addressed during the first experiment. Specifically, to what extent do gravitational forces drive upward migration of the plume? How much CO_2 remains trapped as a residual phase? How much CO_2 dissolves in the brine as it migrates upward under buoyancy forces? Where does the displaced water go? To the extent possible, the experiment will take advantage of baseline data collected as part of the first test.

For this test, CO_2 will be injected into a deeper part of the C sand. After injecting a small amount of CO_2 (the precise volume will be determined by modeling studies), migration of the plume will be tracked for a period of up to a year or more, allowing observations of the extent to which gravitational forces drive the plume upwards and the extent to which the CO_2 remains trapped a residual phase. A combination of well logs, and geophysical imaging will be used to track migration of the CO_2. Fluid samples will be collected to determine the extent of CO_2 dissolution in the brine. In addition, fluid sampling will be used to track migration of the displaced water. The role of our team will be to:

- Continue to refine interpretation of the Frio I test data to improve the knowledge gained from this test and to improve MMV methods;
- Help identify the optimal suite of MMV technologies to deploy by using our forward and inverse geophysical simulator;

- Deploy unique capabilities such as the U-tube sampler, multi-level sampler, noble gas tracers, and potentially, the P- and S- wave seismic source; and
- Participate in the integrated interpretation and simulation of the fate and transport of the injected CO_2.

Task 1 Results and Discussion

Geophysics

Data analysis of the Frio site crosswell and VSP data has continued. Analysis of the VSP data was refined with more accurate spatial mapping of the observed CO_2 induced changes. These changes, mapped on three azimuths from the injection well, compared favorably to the expected CO_2 saturation predicted by flow models. Analysis of the crosswell amplitudes has begun, including initial finite-difference modeling. Initial estimates of partial CO_2 saturation derived from field measurement of velocity changes were accomplished. Analysis of ambient borehole seismic 'noise' using the time-lapse crosswell data shows potential for monitoring changes in fluid motion in the borehole annulus. Collaboration on analysis of the VSP data was begun with Schlumberger. Collaboration on analysis of the crosswell data was begun with MIT. Results were presented at the annual meetings of the Society of Exploration Geophysicists, and the American Geophysical Union. Additionally, initial planning for the second Frio injection experiment has begun. A more detailed discussion on the use of seismic noise for locating flow behind the casing is presented below.

Seismic Noise Analysis from the Cross-well Data Collected at the Frio Brine Pilot

Acoustic noise studies in wells for the purpose of characterizing out-of the casing fluid flow was a subject of intensive studies in the past. The results suggested possibility of multi-fluid flow detection and recognition using noise spectra in 0-5 KHz range. Although the noise studies were not initially planned for the CO_2 injection experiment, we later included noise analysis as it seemingly contained interesting information. Noise records were obtained by extracting the 0.25-0.4 s interval from the 0.5 s long traces to avoid influence of source related direct body waves. Figure 1 shows an example of pre- and post- shot gathers for 5000 ft source depth. Visible are increased noise at 5030-5060 ft (injection) and 4950-5000 ft depth intervals in post-injection gather. These high noise depth ranges are present at all source gathers which means that they are not related to any specific source position. However, a substantial part of the noise might be caused by the seismic source because of multiple scattering of wave energy in the formation and because converted tube waves generally have low attenuation.

Noise amplitude spectra (Figure 2) show visible amplitude peaks at 80 Hz and at 380 Hz. The 380 Hz peak is stronger than 80 Hz peak for pre-injection data while this relationship reverses for the post- data. This might be because of higher attenuation of the primary body waves in gas saturated rocks. While there is no other significant depth related features for source gathers (although there is some increase in amplitudes at 188-170 Hz for 4940-4990 ft interval), there is a distinctive change for injection well (5030-5060 ft

interval) level and for 4950-4990 ft interval. These indicate that the location of the source noise is likely close to the injection (receiver) borehole. At high frequencies (350 Hz) post injection amplitudes are about three times lower than pre- injection amplitudes for all depths (Figure 3). At lower frequencies the average noise levels for post- and pre-injection amplitudes are comparable. Combined plots of all source-receiver pairs (Figure 4) show two distinctive peaks of noise amplitudes for injection (5030-5060 ft) interval and for 4950-4990 ft interval and confirm that high noise sources are located close to the injection (receiver) borehole.

In a search for phase flow signatures the noise amplitudes were computed along the injection (receiver) well at different frequencies (Figure 4). Amplitude dependence on frequency for the 4950-4990 ft interval shows steady decrease as frequency becomes higher corresponding to two-phase flow pattern. The amplitude distribution for the injection interval shows highest peak at intermediate frequencies possibly indicating presence of both one-phase and two phase flows. This interpretation can be more conclusive if we had higher frequencies in data (at least up to 2 KHz). Currently, traces have frequencies up to 420 Hz.

Seismic noise in fluid-filled boreholes is primarily represented by vertically propagating tube waves. Tube waves have low attenuation and their velocities are usually below 1500 m/s. To evaluate the local apparent velocities of the noise-forming waves we computed cross-correlations of neighboring noise traces (Figure 5). The result of such computation gives local measurements of (tube) wave velocities, which are sensitive to rock properties behind the casing and to a quality of casing contact with rock formation. For a homogeneous media these plots would have distinct vertical stripe pattern. Deviations from this pattern indicate changes in the well casing surrounding. The largest distortions are observed at 5000 ft depth zone. Although the dependence of the obtained images on depth turned out to be rather complex, the shape of the cross-correlation curves seems to be rather sensitive to the noise source. Figure 6 shows a correlation coefficient between cross-correlation curve at reference depth of 4500 ft and cross-correlation curves from Figure 5 computed for other depths. Deviation of these curves from value one indicates that at this depth the acoustic noise has components other than tube waves, which means that the peaks point on the actual depths where the noise is generated. Remarkably the pre-injection curve gives the largest peak at 4950 ft before the injection, possibly indicating a presence of a faulty bonding between casing and the formation. This curve also points at" the injection (reservoir) 5050 ft. If proven robust such measurements can give locations of weak zones behind a casing before the injection stage.
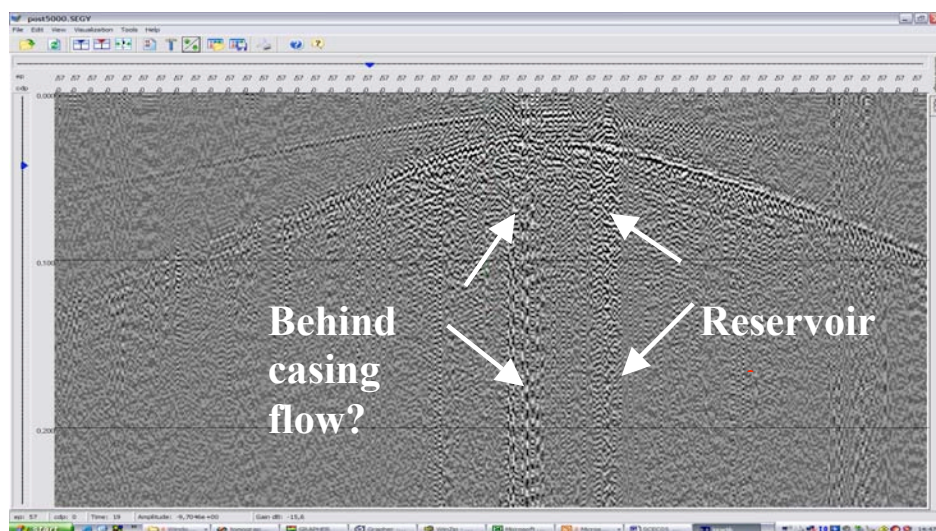
The results of the Frio CO_2 seismic noise study suggest the presence of the two-phase flow at 4950 ft depth (approximately 80 ft above the reservoir) after the injection. This hypothesis will be tested by evaluating pre-and post-injection well logs, and perhaps, by collecting new data specifically for this purpose.
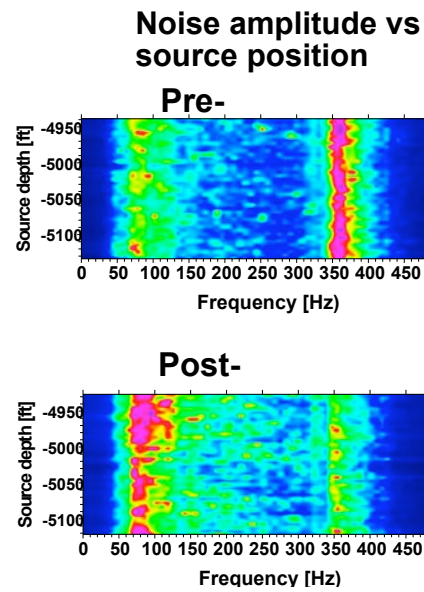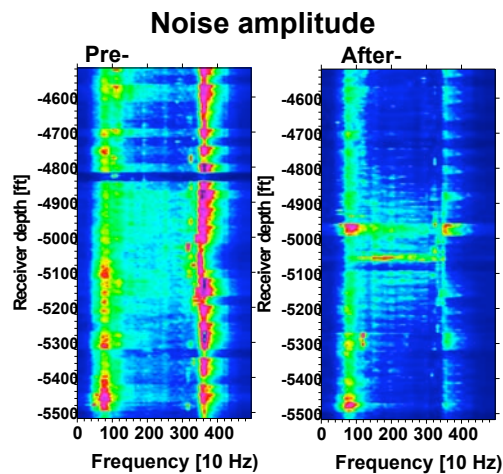
(a)
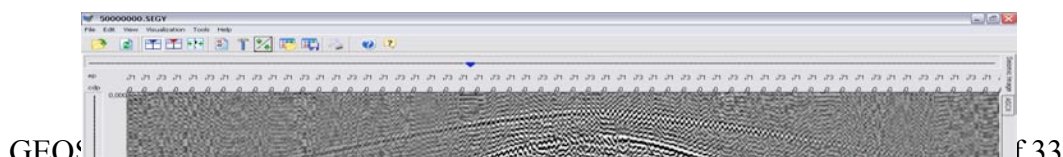
(b)

Figure 1. Seismic cross-well pre- (a) and post- (b) shot gathers for 5000 ft source depth for Frio CO_2 injection experiment. Visible are increased noise at 5030-5060 ft (injection) and 4950-5000 ft depth intervals in post-injection gather.

(a)

Noise amplitude vs source position

Pre-

Post-


(b)

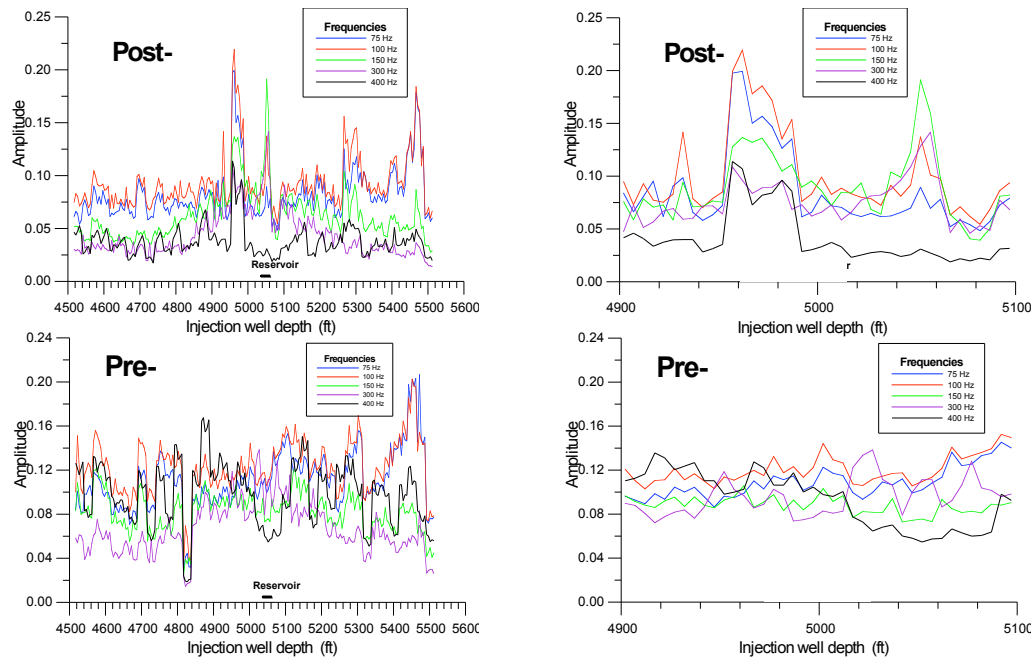**Noise amplitude**

Pre-   After-

Figure 2. Noise amplitude spectra vs. source depth (a) and receiver depth (b) for pre- and post-injection. Visible are amplitude peaks at 80 Hz and at 380 Hz. The 380 Hz peak is stronger than 80 Hz peak for pre- data while this relationship reverses for the post- data. While there is no other significant depth related features for source gathers (note some increase in amplitudes at 188-170 Hz for 4940-4990 ft interval), there is a distinctive change for injection (5030-5060 ft interval) level and for 4950-4990 ft interval. These results indicate the location of source noise in the close proximity of injection (receiver) borehole.
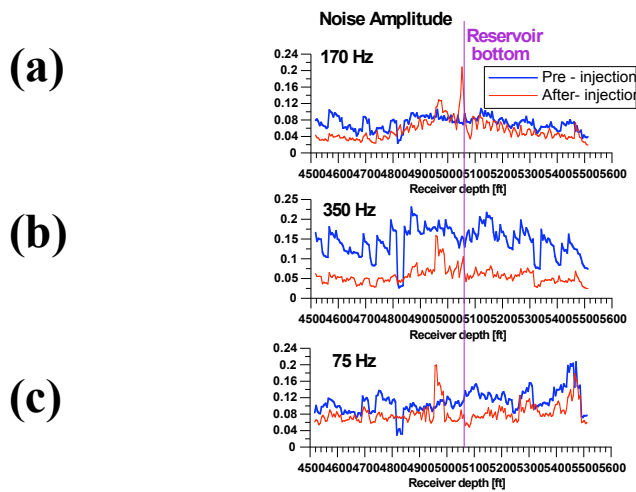
Figure 3. Noise amplitude spectra vs receiver depth for pre- (blue line) and post- (red line) injection at 170 Hz (a), 350 Hz (b), and 75 Hz (c). Reservoir level (5030-5060 ft interval) is clearly marked by a sharp peak at 170 Hz. In the 4940-4990 ft interval has clear peaks at all frequencies. At high frequencies (350 Hz) post injection amplitudes are about three times lower than pre- injection amplitudes for all depths. At lower frequencies the average noise levels for post- and pre- injection amplitudes are comparable.
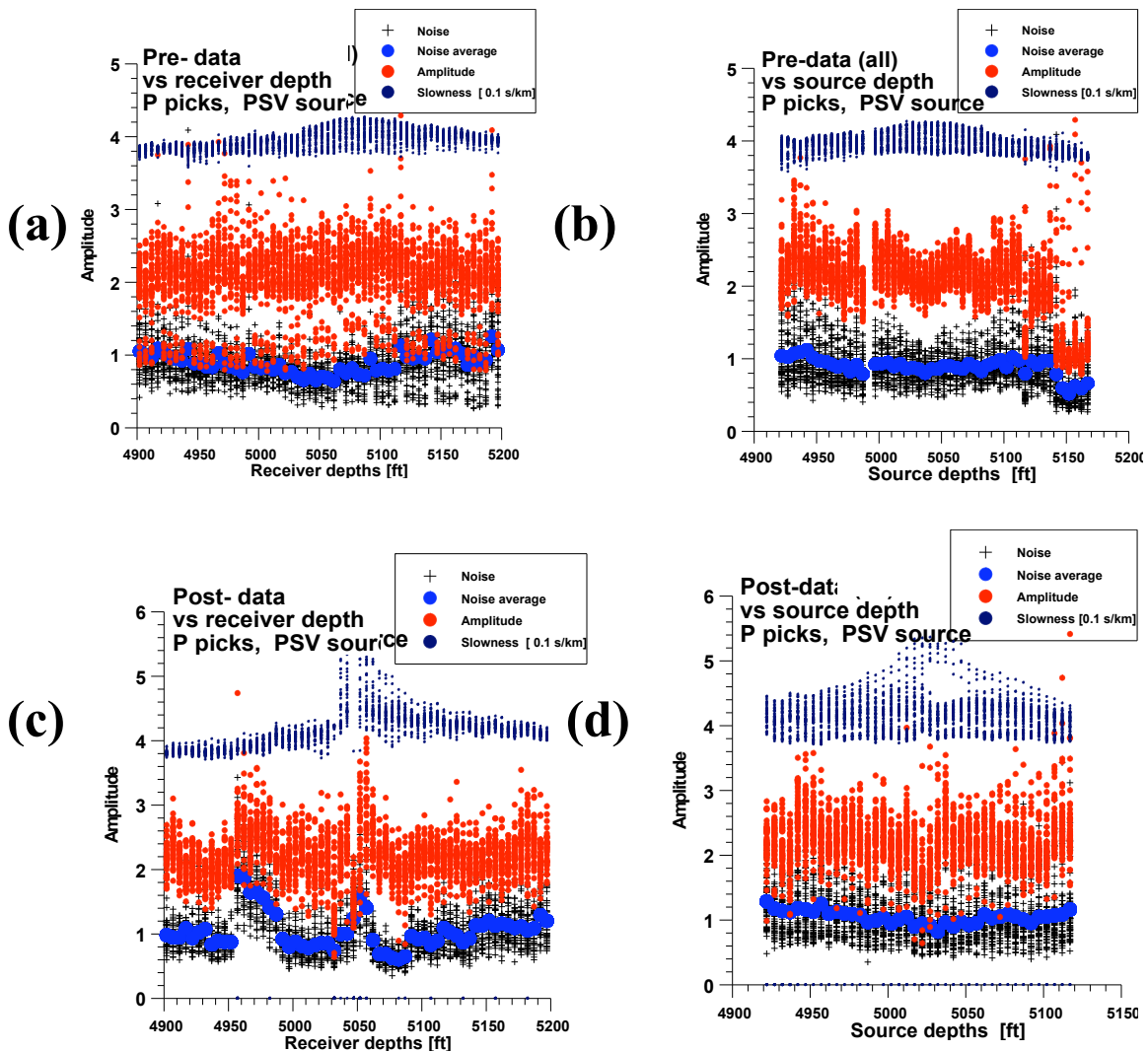
Figure 4. Combined plots of cross-well Frio CO_2 injection data for all source-receiver pairs. Panels (a) and (b) show pre-injection results, while panels (c) and (d) show post-injection results. Left panels correspond to the data assembled along the receiver depths, and right panels show the data assembled along the source depths. Small black dots are the slownesses picks for the first arriving P- wave. Red dots show amplitudes of the first arriving P-waves. Black crosses show noise amplitudes for the whole spectral range. Blue dots ate the average values of noise amplitudes. Distinctive are two-fold rises of noise amplitudes for injection (5030-5060 ft) interval and for 4950-4990 ft interval. These results similar to Figure 2 indicate the location of source noise in the close proximity of injection (receiver) borehole.

Figure 5. Noise amplitudes along the injection (receiver) well at different frequencies for pre- (bottom panels) and post- (upper panels) injection surveys. Set of frequencies includes: 75 Hz (blue lines), 100 Hz (red lines), 150 Hz (green lines), 300 Hz (violet lines), 400 Hz (black lines). Left panels show whole range (4500-5500 ft) of receiver depths, while right panels show same data for 4900-5100 ft depth interval. Amplitude peaks on upper (post-) panels correspond to the injection (5030-5060 ft) interval and to the 4950-4990 ft interval. Amplitude dependence on frequency for this interval shows steady decrease as frequency becomes higher corresponding to two-phase flow pattern. The amplitude distribution for the injection interval shows highest peak at intermediate frequencies possibly indicating presence of both one-phase and two phase flows. This interpretation can be more conclusive if we had higher frequencies in data (at least up to 2 KHz). Currently, traces have frequencies up to 420 Hz.
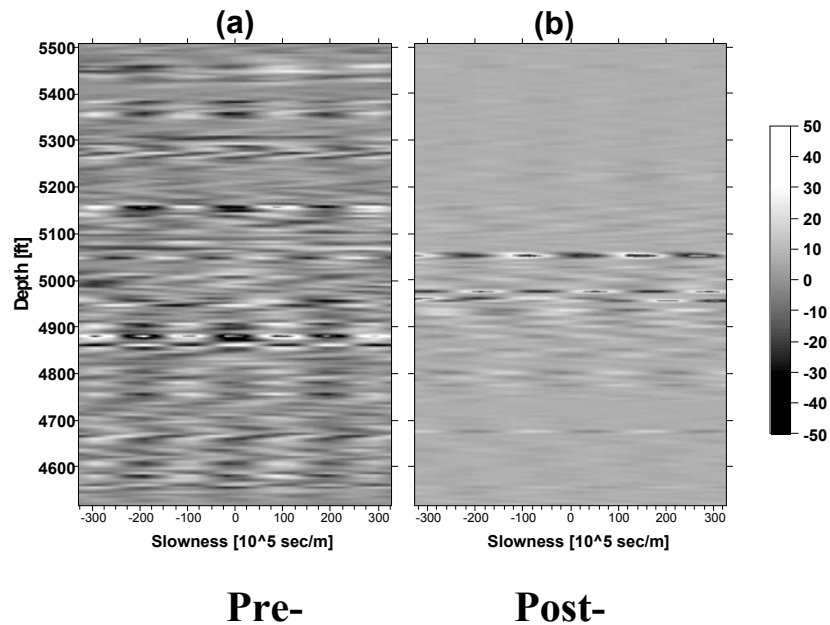
Figure 6. Cross-correlation of neighboring noise traces (velocitygramm) for pre-injection (a) and post- injection (b) data. Horizontal axis is scaled to have slowness units 10^5 s/m. Closest to zero slowness maximums correspond to tube wave velocities. Other maximums are likely the result of aliasing because of sparse vertical receiver spacing. These plots give local measurements of tube wave velocities, which are sensitive to rock properties behind the casing and a quality of casing contact with rock formation. For a homogeneous media these plots would have distinct vertical stripe pattern. Deviations from this pattern indicate changes in the well casing surrounding. The largest distortions are observed at 5000 ft depth zone.
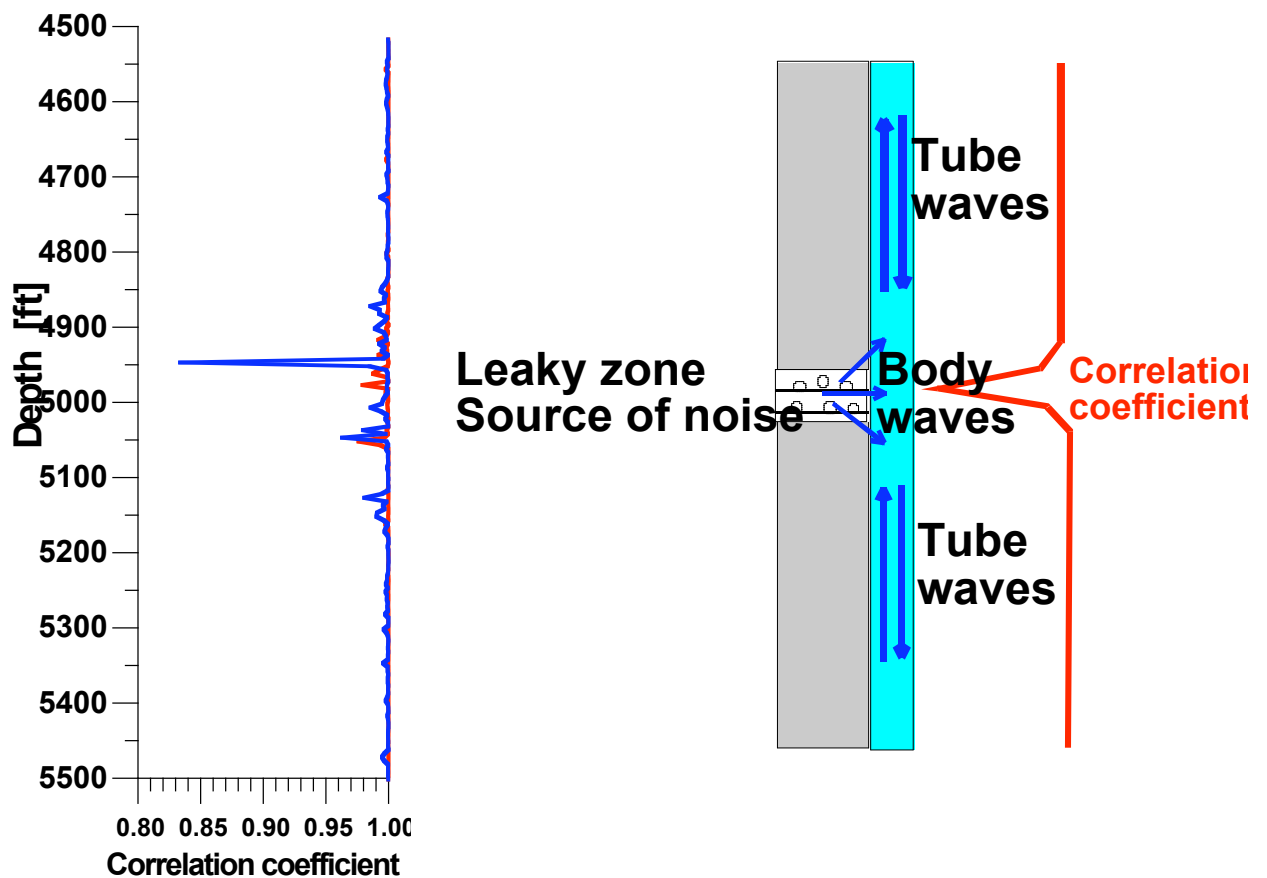
Figure 7. *Left panel.* Correlation coefficient between cross-correlation curve at reference depth of 4500 ft and cross-correlation curves from Figure 5 computed for other depths. Blue line shows pre- data and red line shows post- data. Deviation of these curves from value one indicates that at this depth the acoustic noise has components other than tube waves. In other words the peaks on this figure point on the actual depths where the noise is generated. Remarkably the blue (pre-) curve gives the largest peak at 4950 ft before the injection, possibly indicating a presence of a faulty bonding between casing and the formation. This curve also points at" the injection (reservoir) 5050 ft. If proven robust such measurements can give locations of weak zones behind a casing before the injection stage.

Right panel. Explanation of correlation anomaly caused by a local noise source. Body waves enter into the well space a variety of incident angle in a close proximity to the source. At some short distances from the source they convert into tube waves propagating along the well.

Modeling studies in conjunction with the Frio brine pilot

Numerical modeling of the flow behavior of supercritical carbon dioxide (CO_2) injected into a brine-bearing sandstone was an integral part of the Frio brine pilot for CO_2 sequestration. Modeling was used to help design the pilot and to improve understanding of multi-phase and multi-component flow processes involved in geologic CO_2 sequestration. During the design phase, modeling was used to determine which of several layers to inject into, how far apart injection and observation wells should be (in particular showing that existing wells were too far apart, necessitating the drilling of a new injection well), how much CO_2 to inject, and at what rate. Modeling of pre-injection, site-characterization pump and tracer tests helped design these tests to optimize the information gained on formation flow properties, in situ phase conditions, and boundary conditions. As site-characterization proceeded, the model was modified to incorporate new information. CO_2 injection was simulated prior to the actual pilot, to assess the model's predictive ability. Further model improvements were added subsequently, based on detailed comparisons to the observed subsurface CO_2 distribution.

Modeling illustrated the complex interplay between phase interference and buoyancy flow that occurs as CO_2 is injected into a high-permeability, steeply dipping sand layer. By running simulations with a range of parameters and comparing model results to field data we improved our understanding of these flow processes. Generally good agreement between observed and modeled CO_2 spatial distributions and travel times between injection and observation wells validated our ability to model CO_2 injection, while discrepancies pointed out areas where future research is needed. The iterative sequence of model development, application, and refinement proved useful for getting early results in a timely manner as well as incorporating more complexities at later stages. This work has demonstrated that we have an effective modeling capability for representing the physical processes occurring during CO_2 sequestration in brine-bearing sandstones, and moreover that the incorporation of modeling into geologic CO_2 sequestration activities is beneficial from the earliest design stages through the final interpretation of field data.

Comparison of ECO2 with ECO2N
The majority of the Frio brine pilot modeling studies employ the TOUGH2 equation of state package ECO2, which has been in use for several years. A new, more comprehensive equation of state package, denoted ECO2N, has recently been developed, superceding ECO2 as the standard equation of state package for modeling CO_2 in saline aquifers. Comparison of results obtained using ECO2 and ECO2N show only minor differences in the formation and evolution of CO_2 plumes for the conditions of the Frio brine pilot.

Analysis of the Effects of Hysteretic Characteristic Curves on Interpretation of the Frio Brine Pilot
TOUGH2 has had the capability of using hysteretic relative permeability and capillary pressure curves for many years. Hysteretic capillary pressure functions were introduced in the late 1980's and hysteretic relative permeability functions were added about ten years later. Until recently, however, the hysteretic version of TOUGH2 has not been

numerically efficient enough to be used for 2D or 3D CO_2 sequestration problems. Recent modifications have improved the numerics, making it computationally competitive with non-hysteretic simulations.

The use of hysteretic characteristic curves is not so critical for the simulation of CO_2 injection periods when the plume is continuously growing, because the entire model is following the primary drainage branch of the capillary pressure curve, and this branch can be replicated using a non-hysteretic formulation. However, for post-injection periods, as the plume moves upward and updip due to buoyancy forces, different locations experience drainage and wetting at different times, necessitating the use of a hysteretic formulation.

New simulations have been done to evaluate the effect of hysteretic characteristic curves on the pilot test have been carried out.

Comparison of Frio I Simulations with Observed Data
Figure 8 shows several views of the three-dimensional grid used for the Frio I modeling studies. The grid is created as a stack of 13 flat layers, then tilted to account for dip. Vertical grid spacing is chosen to resolve geological variability in the upper part of the C sand, as observed in well logs (Figure 9). Lateral grid spacing is finest near the two wells, and gets coarser farther away.
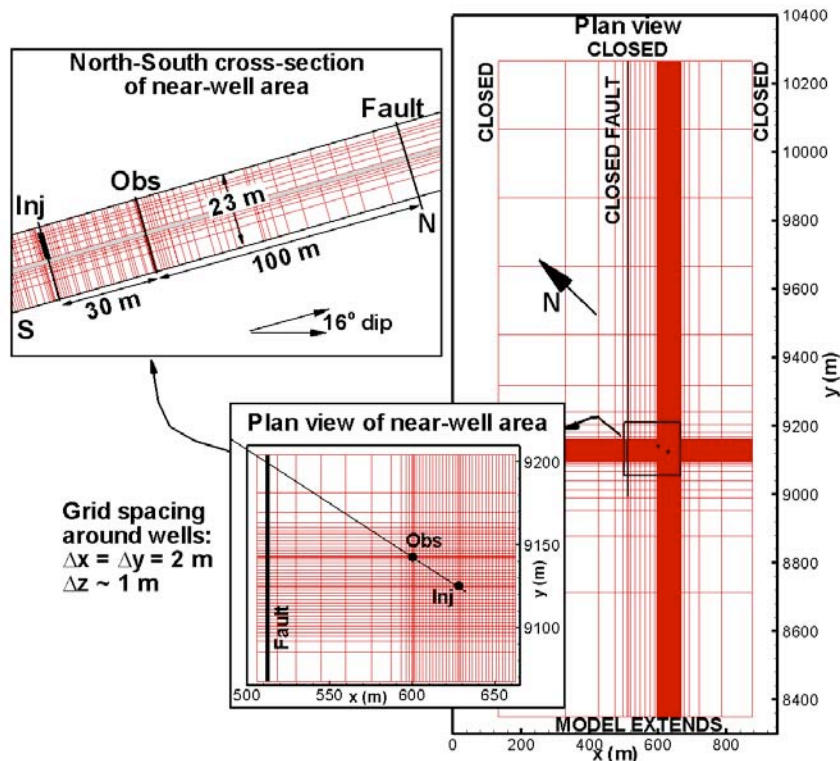

Figure 8. Three-dimensional grid used for modeling the Frio I brine pilot.
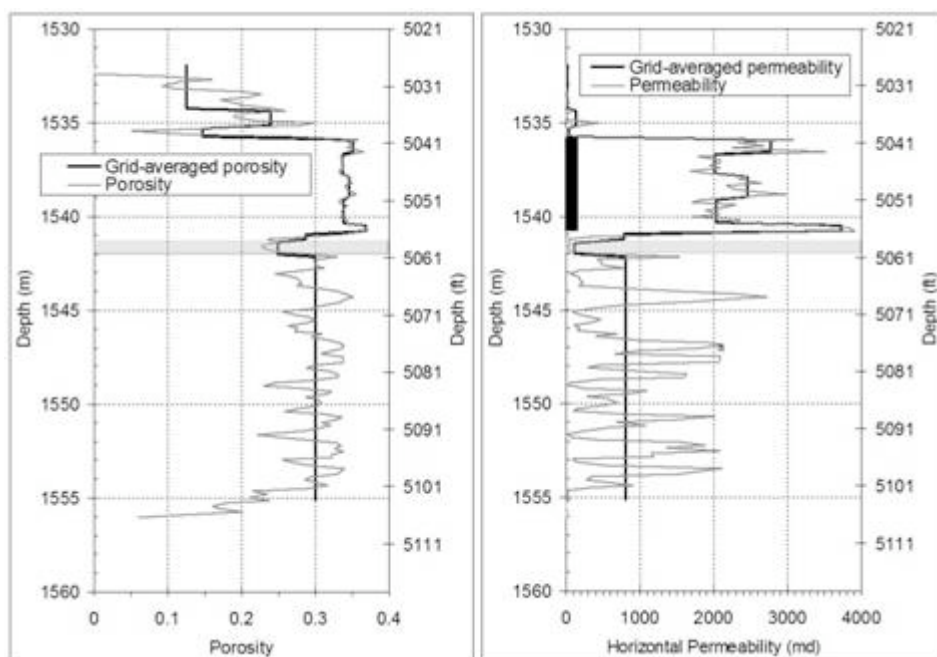
Figure 9. Porosity and permeability profiles inferred from injection-well logs and core sample analysis, and grid-averaged values used for the model. The perforated interval is also shown. Geologic variability is not resolved below the thin low-permeability marker bed (shown with gray shading).

During the Frio I pilot (October 2004), sampling from the U-tube indicated that free-phase CO_2 arrived at the observation well 51 hours (2.1 days) after injection began, somewhat earlier than the model prediction of 3 days, made with the non-hysteretic TOUGH2 prior to the field test (Figure 10). Subsequent modeling using the hysteretic TOUGH2 produced a CO_2 arrival at 2.2 days. The hysteretic formulation uses a zero value of residual gas saturation for drainage, the dominant process occurring during the 10-day CO_2 injection period, whereas the non-hysteretic formulation used a small but non-zero value, resulting in a greater mobility of the gas phase for the hysteretic case, which enables more gravity override, and hence a shorter travel time from the injection well to the observation well.
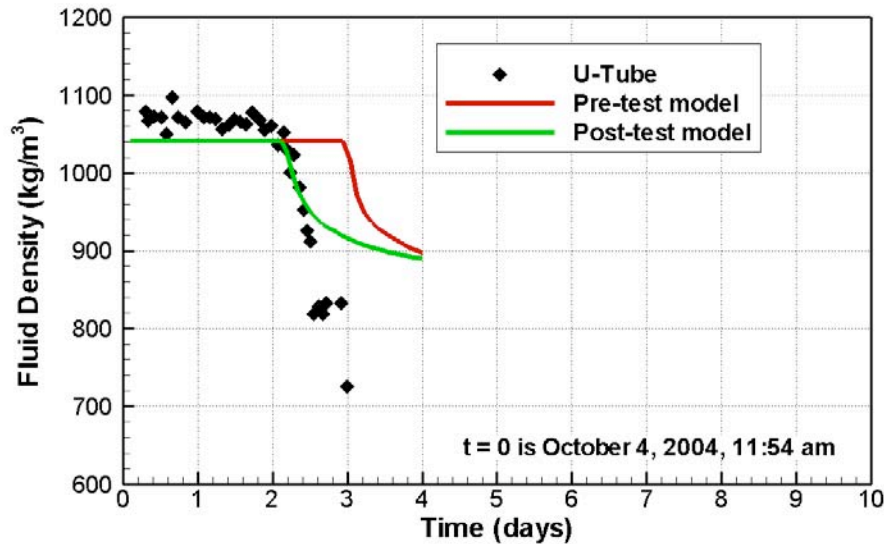
Figure 10. Observed and modeled CO_2 arrival at the observation well. The pre-test model is non-hysteretic whereas the post-test model uses a hysteretic formulation for characteristic curves.

Schlumberger's RST tool was used to produce CO_2 saturation profiles at the injection well and observation well at a series of times during and after the Frio I CO_2 injection, as shown in Figure 11. Model results at the injection well compare favorably with the RST profiles, whereas model results at the observation well show a CO_2 plume that is about one meter too low. Figure 11 shows that the upper limit of the CO_2 plume in both wells is aligned with the upper limit of significant porosity (right-hand panel). In the injection well, the model reproduces this part of the actual porosity profile nicely, whereas in the observation well the modeled top of the high-porosity interval is about one meter too low. This finding suggests that either the Frio formation dips more steeply than the assumed 16 degrees, or that the upper boundary of the C sand is not a sharp, continuous low-permeability layer. The latter assumption was tested by replacing part of the 0.61-m thick, low-permeability layer above the injection interval with a high-permeability sand, with the sand extending laterally from about midway between the injection and observation wells to beyond the observation well. This modification produced the desired upward shift in CO_2 arrival at the observation well, without altering the CO_2 distribution at the injection well.

Figure 11 also shows that the extent of the CO_2 plume below the perforated interval in the injection well is slightly greater than that predicted by the model, suggesting that the thin marker bed located below the perforated interval may not have as low a permeability as assumed. These model modifications based on the CO_2 distribution illustrate the iterative nature of model development and application. The strong preferential flow exhibited by the low-viscosity, low-density CO_2 plume provides a powerful tool for site characterization.
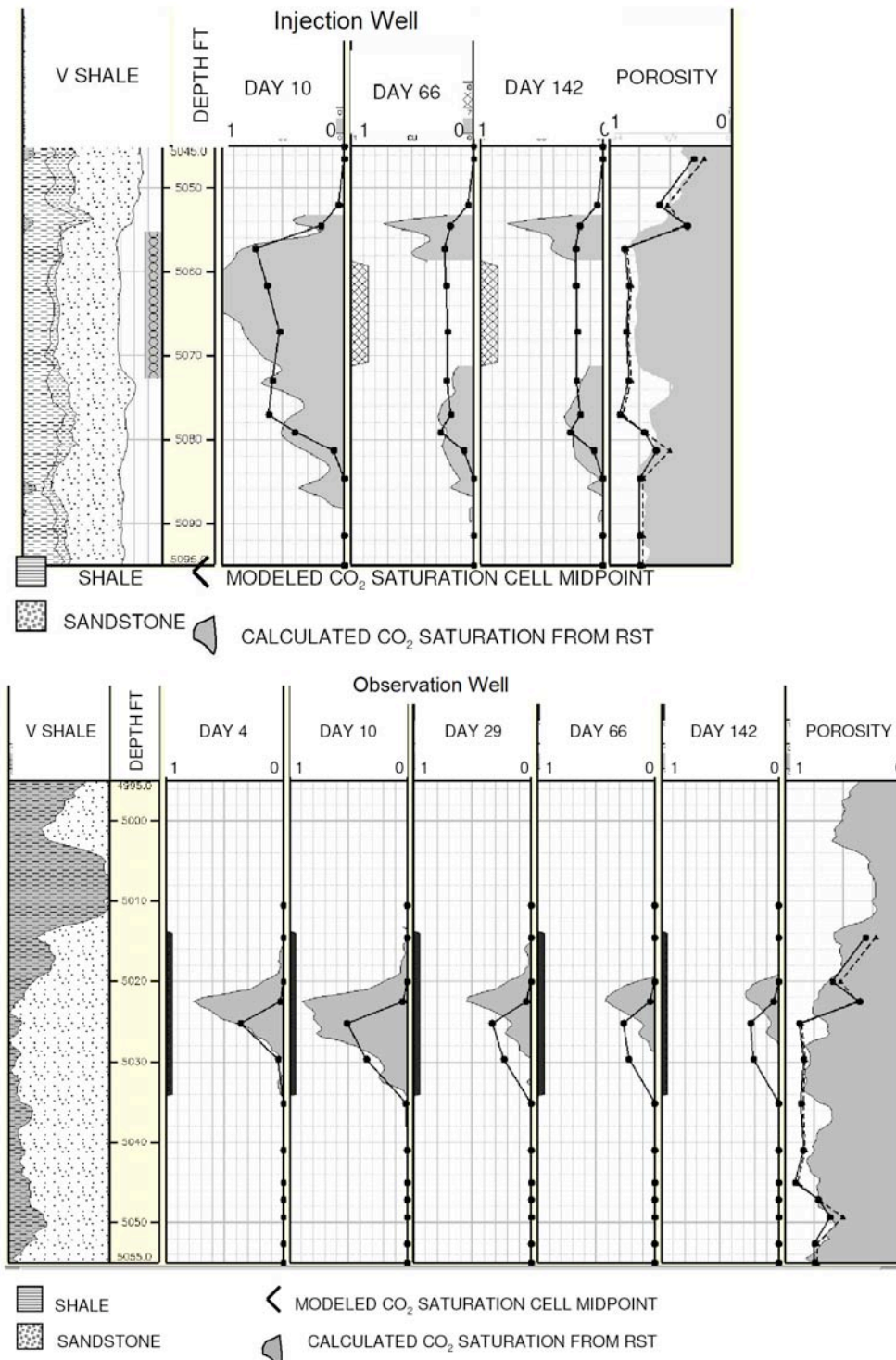
Figure 11. Observed and modeled CO_2 saturation profiles in the injection well (top) and observation well (bottom). At the perforated interval in the injection well, day 66 and day 142 RST data cannot be processed, due to operational changes made to the well at the end of injection period. The right-hand panel shows porosity inferred from the well log's Vshale (gray shading) and grid-averaged values (black lines).

Figure 12 compares the difference tomogram obtained from two crosswell seismic surveys conducted prior to and about six weeks after the Frio I injection of CO_2 with model results for the CO_2 distribution along the vertical cross-section between the injection and observation wells. We do not have a quantitative relationship between velocity change and CO_2 saturation, but there is excellent qualitative agreement between the model and the tomogram for the CO_2 distribution in the inter-well plane.
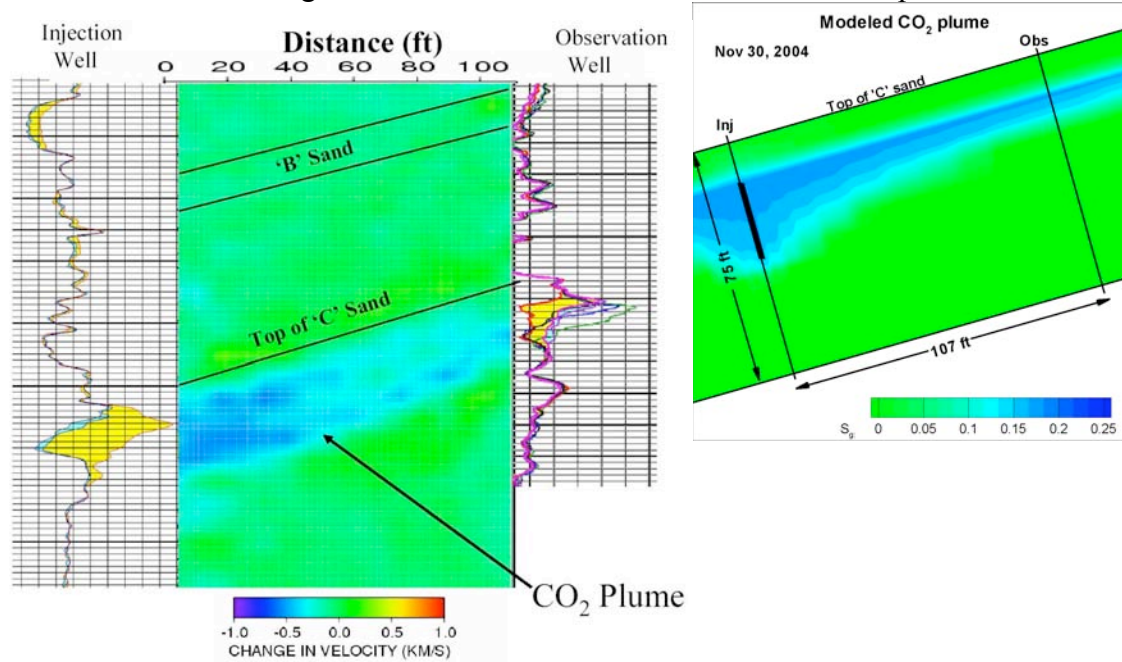
Figure 12. Velocity difference tomogram with saturation profiles in the wells obtained from RST (left) and modeled CO_2 distribution (right).

Figure 13 compares vertical seismic profile (VSP) results for the far field CO_2 distribution about six weeks after the Frio I pilot with model results. As for the crosswell seismic, we do not have a quantitative relationship between VSP change in amplitude and CO_2 saturation, so the vertical axes of the plot are adjusted to align these two quantities close to the injection well. Figure 11 shows good agreement between model and VSP in the updip direction (N), but the VSP indicates that the plume has moved farther than the model has predicted to the NE and NW. In fact, the plume has moved as far to the NW as it has to the N, suggesting that either our notion of the true dip direction is inaccurate, or that there is significant heterogeneity or anisotropy in the permeability distribution beyond the immediate vicinity of the wells. The non-smooth nature of the model profiles far from the injection well indicates the need for a more refined grid.
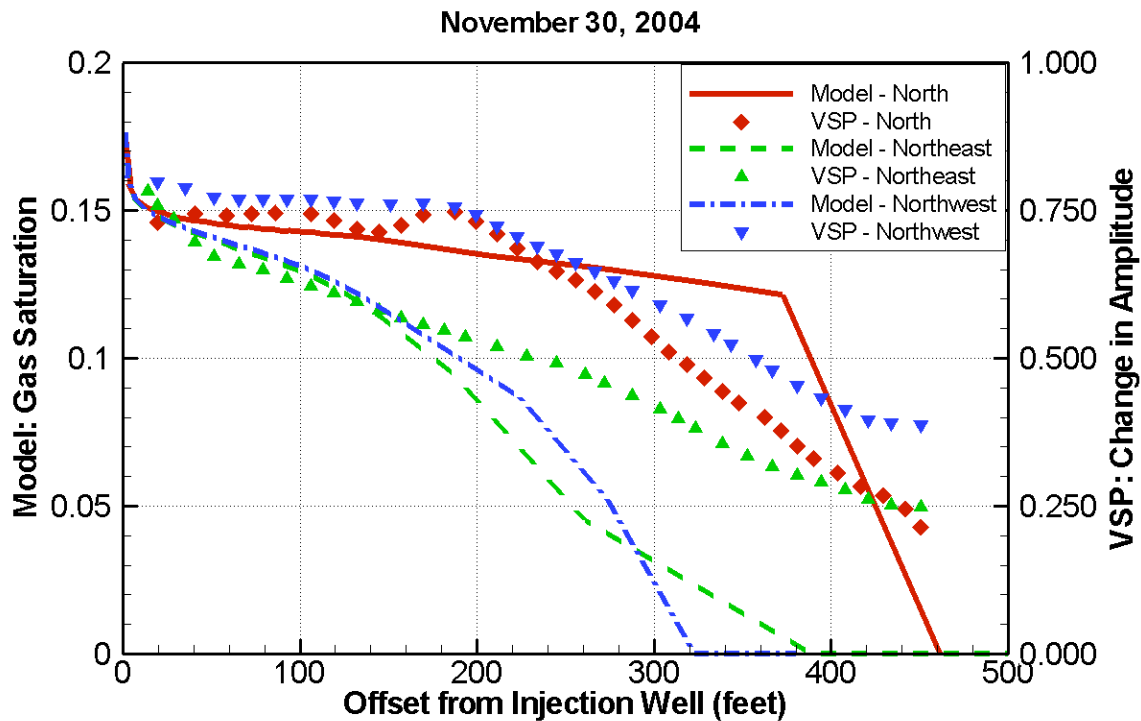
Figure 13. Comparison of VSP and model results for far-field CO_2 distribution.

Scoping studies for Frio II

Frio II, the second stage of the Frio brine pilot, is in the preliminary design stage. The goal is to inject a small plume of CO_2 in a location where it can move upward under buoyancy flow. Two locations are being considered: the lower part of the C sand (below the thin low-permeability marker bed, see Figure 9) and a deeper sand known as the 5400 sand. Figure 9 indicates that unlike the upper C, where there is a 5-m thick layer of very high permeability (>2000 md) sand, in the lower C, thin high- and low-permeability layers alternate. Hence, buoyancy flow is expected to be less pronounced.

Table 1 summarizes the issues addressed by the first round of scoping studies to aid in the design of Frio II. The model used for the studies is similar to the one used for Frio I (Figure 8) except that 22 layers are used in order to resolve geologic layering throughout the C sand and lateral grid resolution is not as good (about 5 m grid spacing near the wells). Because calibrated porosity and permeability profiles are not available for the 5400 sand, the C sand model is used for these studies as well, but with pressures and temperatures increased as appropriate for the greater depth. Thus at this preliminary stage, the only issue to be tested for the 5400 sand is how the pressure- and temperature-dependent properties (density and viscosity of CO_2 and brine) affect the plume formation and evolution.

Table 1. Issues considered for preliminary scoping studies for Frio II.

Issue	Options	Comments
Depth to inject	Lower C sand	Pro: geology already characterized via well logs calibrated to core samples. Con: new plume might interfere with existing plume (injected in upper C sand).
	5400 sand	Pro: no existing CO_2. Con: well-logs not yet calibrated to core samples.
Rate to inject	Same as Frio I (~160 T/day) or less	Want slower arrival. Rate may be limited by pressure increase (if permeability of 5400 sand is much lower than C sand).
Volume to inject	800 T or less	Ideally would like arrival reasonably soon after injection is stopped. Limited by high cost of CO_2.
Time duration of injection	10 days or less	Limited by high cost of field time.

During Frio I, CO_2 arrived at the observation well during the injection period, when plume evolution was dominated by forced convection. For Frio II, we would like to inject a small enough volume so that arrival does not occur until after injection has ended, so we will be monitoring a period of natural convection. The risk of CO_2 not reaching the monitoring well is much greater in this case however, because as soon as injection ends, the problem shifts from a drainage-dominated problem (plume continuously growing), to a problem combining drainage (at the leading edge of the plume) and wetting (at the trailing edge of the plume). For the wetting process, the residual gas saturation can be quite large, effectively immobilizing the plume.

Tables 2 and 3 summarize the scoping simulations completed so far. Each lower C sand simulation begins with the Frio I simulation (October 2004), then rests until March 1, 2006, which provides the initial conditions for the Frio II simulation.

Table 2. Preliminary scoping calculations for Frio II.

Case	Features	Comments
G05	Same rate and duration as Frio I (~1600 T in 10 days), inject at bottom 1.4 m of C sand	CO_2 arrival 2.67 days – comparable to Frio I
G05-5400	Like G05, but at 5400' depth	CO_2 arrival 2.73 days – nearly unchanged from G05
G05A	Like G05, but half injection rate	CO_2 arrival at 4.5 days – halving injection rate increases but does not double arrival time
G05B	Like G05A, but spread injection over lower 3 m of C sand	CO_2 arrival at 5.7 days –longer arrival time for thicker plume
H05A	Like G05A, but all layers more anisotropic: $k_v/k_h=0.1$	CO_2 arrival at 3.5 days –shorter arrival time for less buoyancy flow

Based on the results shown in Table 2, and the goal to slow down the CO_2 arrival at the observation well, a lower injection rate will be advantageous. The pressure and temperature increase for the 5400 sand increase CO_2 density and viscosity just slightly, so have little effect on CO_2 plume evolution. Using a thicker injection interval and considering a more anisotropic medium have modest effects.

The key question is the total amount of CO_2 to inject, or equivalently, the duration of the injection period, which will determine whether injection is still occurring when CO_2 arrives at the observation well. Results of 20-day simulations using three different injection periods are shown in Table 3. Another parameter varied for the calculations is the value of maximum residual gas saturation S_{grmax}. Values from the Gulf Coast petroleum literature indicate that $S_{grmax} \sim 0.2$ for the multi-Darcy layers of the C sand, but our only site-specific information on this parameter comes from the late-time RST profiles (Figure 11). For the most, these profiles support large values of S_{grmax}, but in some instances smaller values are suggested. Additionally, operational issues involving well reworking at the end of the injection period made RST data difficult to interpret unambiguously. Because S_{grmax} plays such a large role in the evolution of the CO_2 plume after injection ceases, simulations using two smaller values of S_{grmax} have also been run: a case with literature S_{grmax} values halved, and a case with $S_{grmax} = 0$. The latter case is not expected to be realistic, but provides useful information on limiting behavior.

Table 3. Scoping calculations comparing different amounts of injected CO_2 and different assumptions for S_{grmax}.

Literature values for maximum residual gas saturation		
G05C	160 T: 80 T/day for 2 days	No CO_2 arrival within 20 days – plume immobilized before reaching observation well
G05D	240 T: 80 T/day for 3 days	CO_2 arrival at 9.1 days
G05E	400 T: 80 T/day, for 5 days	CO_2 arrival at 4.6 days – arrival during injection (insensitive to S_{grmax})
Half maximum residual gas saturation		
K05C	160 T: 80 T/day for 2 days	No CO_2 arrival within 20 days – plume immobilized before reaching observation well
K05D	240 T: 80 T/day for 3 days	CO_2 arrival at 7.0 days
K05E	400 T: 80 T/day, for 5 days	CO_2 arrival at 4.5 days – arrival during injection (insensitive to S_{grmax})
Zero maximum residual gas saturation		
J05C	160 T: 80 T/day for 2 days	CO_2 arrival at 12.3 days
J05D	240 T: 80 T/day for 3 days	CO_2 arrival at 6.5 days
J05E	400 T: 80 T/day, for 5 days	CO_2 arrival at 4.5 days – arrival during injection (insensitive to S_{grmax})

The Table 3 results for CO_2 arrival time suggest that injecting for three to four days at 80 T/day, might be a good starting point for further scoping studies. The smaller plume produced by injecting only two days becomes immobilized too easily under realistic conditions of a non-zero value of S_{grmax}, and the larger plume produced by injecting for five days reaches the observation well under forced convection conditions. Figures 14-17 show CO_2 distributions at a series of times for some of the cases. The color shading shows free-phase CO_2 as gas saturation S_g in the plane between the injection and observation wells. The thin low-permeability marker bed is shown as a red line and the single contour line shows the extent of the two-phase region. For each case, the final frame shows the distribution of S_{gr} at one selected time. By comparing the S_{gr} and S_g distributions for that time, one can identify how mobile the CO_2 plume is. Figure 14 shows a complete time series including Frio I and Frio II for case G05C, while Figures 15, 16, and 17 show just the Frio II part of the series for cases G05D, G05E, and K05D, respectively.

Further studies will focus on attempting to constrain values of S_{grmax}, by further analysis of Frio I data and review of the literature.
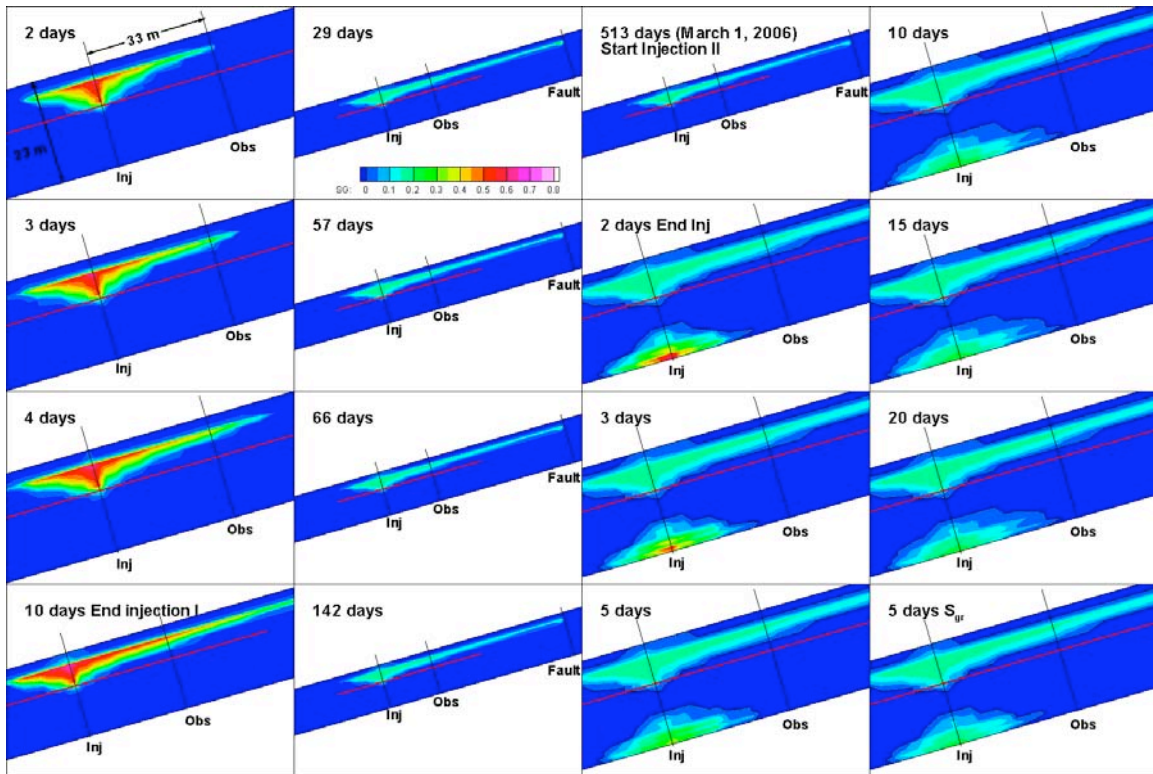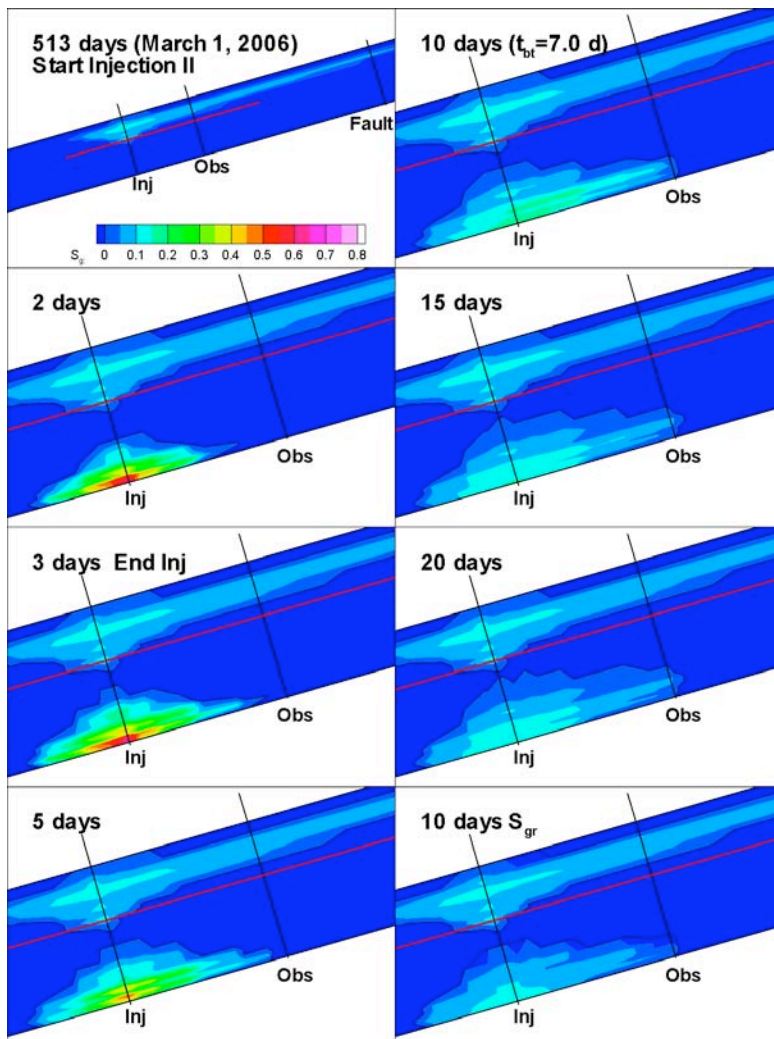
Figure 14. Free-phase CO_2 distributions for a series of times for Case G05C (typical values of S_{grmax}) for Frio I and Frio II (time is re-zeroed at the start of the Frio II injection).
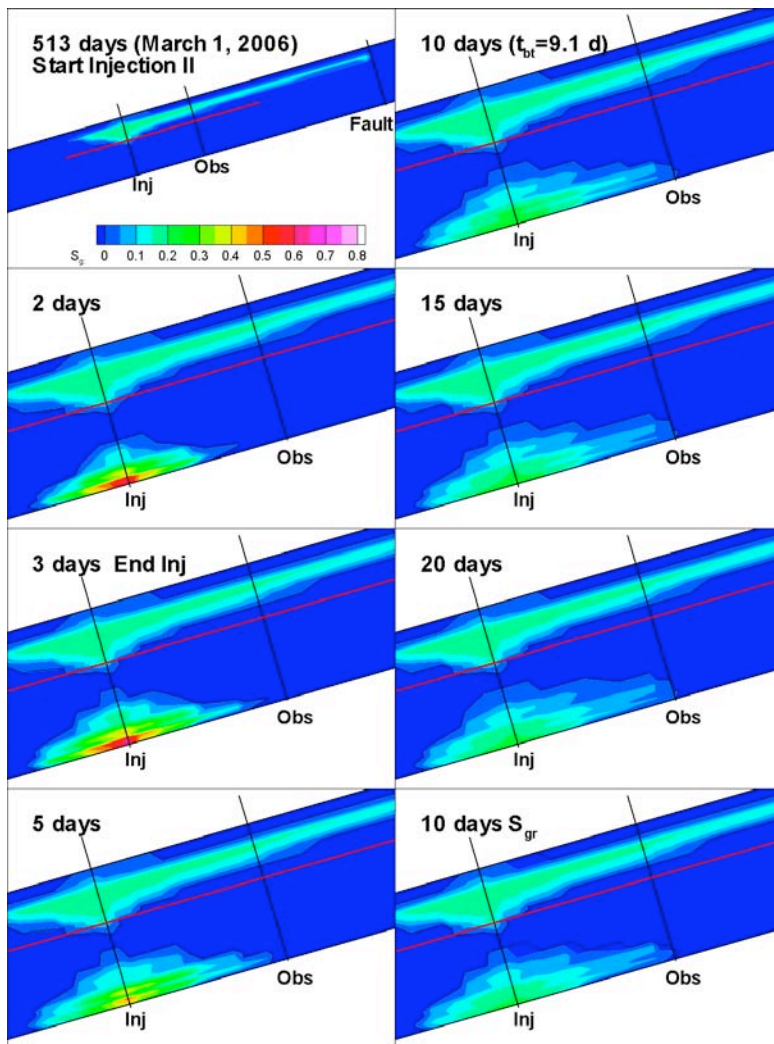
Figure 15. Free-phase CO_2 distributions for a series of times for Case G05D (typical values of S_{grmax}) for Frio II (time is re-zeroed at the start of the Frio II injection).
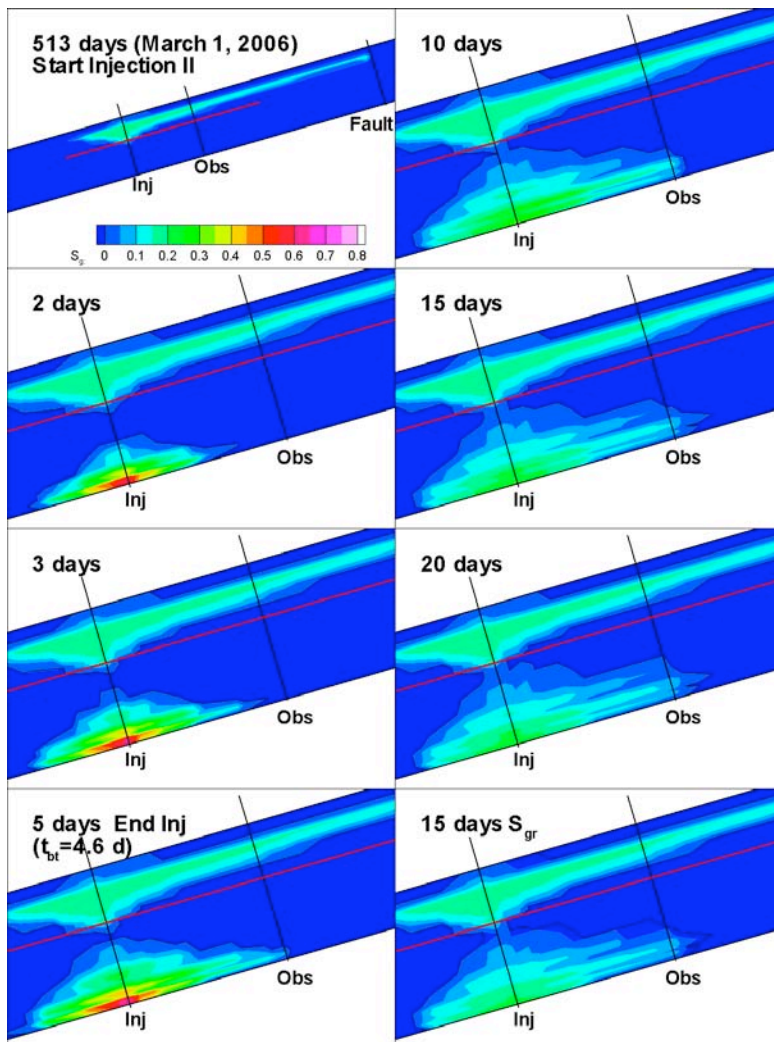
Figure 16. Free-phase CO_2 distributions for a series of times for Case G05E (typical values of S_{grmax}) for Frio II (time is re-zeroed at the start of the Frio II injection).

Figure 17. Free-phase CO_2 distributions for a series of times for Case K05D (half typical values of S_{grmax}) for Frio II (time is re-zeroed at the start of the Frio II injection).

Pressure transient analysis

As part of the Frio Brine Pilot, downhole pressure measurements were obtained from both the injection well and observation well throughout the carbon dioxide injection and recovery phases of the test. In addition, a pre-injection interference test was used to obtain accurate information about the permeability and compressibility of the formation. By comparing the two data sets it is possible to obtain information on field-scale relative permeability during carbon dioxide injection. Analytical techniques have been used to interpret the pressure transient data. In addition, a new inverse approach for deriving field-scale relative permeabilities from pressure transient data has been developed. This is the first time a data set such as this has been collected during carbon dioxide injection into a saline formation. The results provide important insights into the multi-phase flow behavior of carbon dioxide. They also provide important information for predicting the injectivity of carbon dioxide in saline formations.

As a first step in the analysis, the permeability of the formation was measured from single phase pumping and drawdown tests. An example is provided in Figure 18. A number for such tests were made and the interpretation is summarized in Table 4.

During injection of CO_2, the continuous formation pressure measurements shown in Figure 19 were obtained. History matches of these data using an analytical solution are shown in Figures 20 and 21. From this, the relative permeability curves shown in Figure 22 were determined. This new approach for measuring field-scale relative permeability provides a method for quickly assessing a key parameter needed to predict the transport of CO_2 in saline formations.
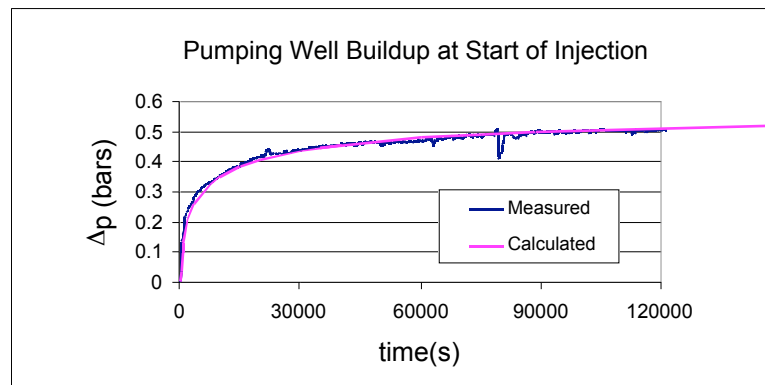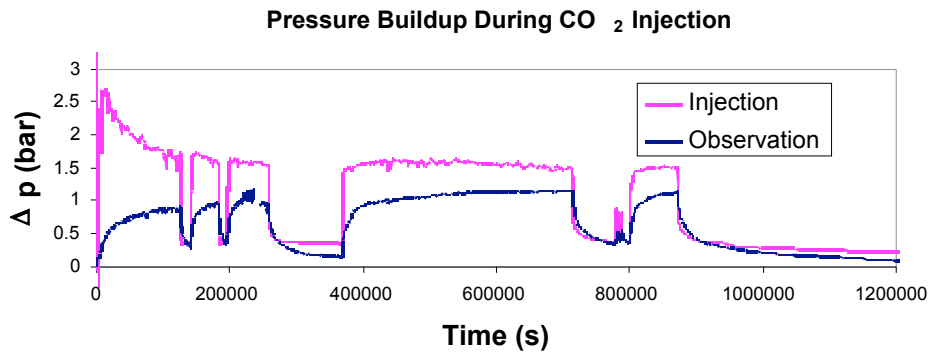

Figure 18. History match between measured and calculated drawdown, resulting in estimates of the formation properties (see Table 4 below).

Table 4. Summary of formation parameters determined from the pre-injection well tests.

| Active Well	Monitoring Well	Test Type	k (m^2)	ϕch(m/Pa)	Comments
Pumping	Injection	Drawdown	2.2x10-12	1.1x10-8	Multi-rate analysis
Injection	Injection	Buildup	2.1x10-12	1.1x10-8	s = 9 Multi-rate, multi-well analysis
Injection	Pumping	Buildup	2.1x10-12	1.1x10-8	Multi-rate, multi-well analysis
Injection	Injection	Falloff	2.1x10-12	1.1x10-8	s=12 Multi-rate, multi-well analysis

Figure 19. Pressure buildup data collected during the CO_2 injection.
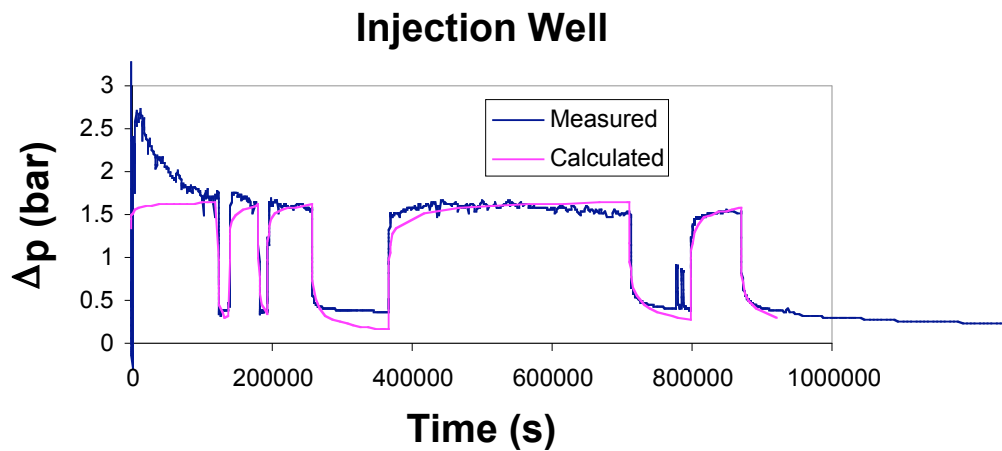
Figure 20. Match between the measured and calculated pressure buildup data at the injection well.
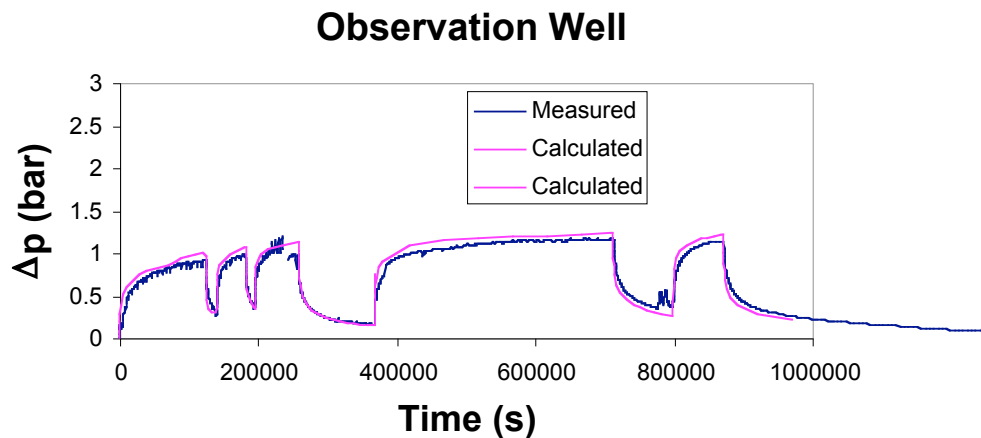
Figure 21. Match between the measured and calculated pressure buildup data at the observation well.

Relative Permeablity
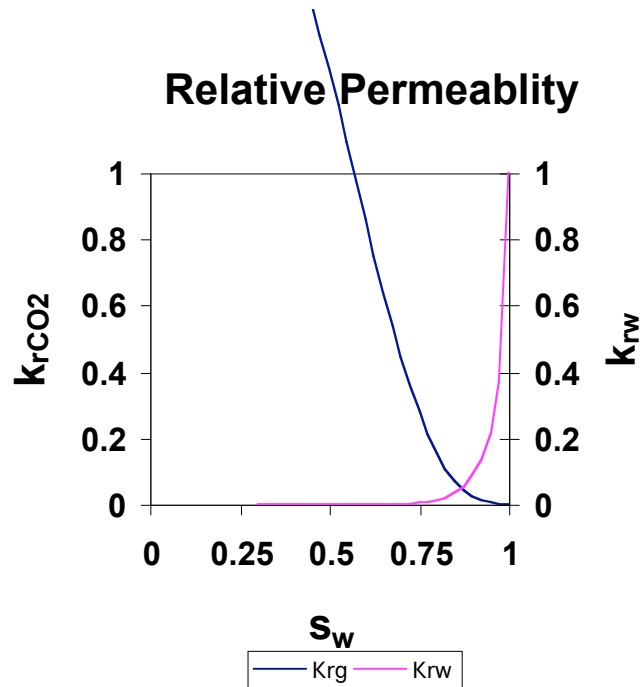
Figure 22. Relative permeability curves determined from the history match of the pressure transient data.

Task 2. Deploy and evaluate MMV and simulation technologies at the Otway Basin Demonstration Site in Australia.

The GEO-SEQ team has been asked to participate in the upcoming demonstration project of geologic storage in the Otway Basin in Australia. This provides a unique opportunity to gain new insights about geologic storage of CO_2 and improve MMV techniques. The demonstration project will take place over a multi-year period and inject up to 100,000 tonnes of CO_2 in gas and saline formations. The comparatively large mass of CO_2 that will be injected, combined with the opportunity to leverage the large investment in this demonstration project by the Australian government and industrial partners, provides a tremendous opportunity for gaining experience with geologic storage of CO_2 in saline formations. The role of our team will be to:

- Help identify the optimal suite of MMV technologies to deploy by using our forward and inverse geophysical simulator;
- Deploy unique capabilities such as the U-tube sampler, multi-level sampler, noble gas tracers, and potentially, the P- and S- wave seismic source; and
- Participate in the integrated interpretation and simulation of the fate and transport of the injected CO_2.

Not only does this test provide a unique opportunity for collaboration, but the injection formation is not unlike many potential storage formations present in the U.S.

Task 2 Results and Discussion

October 2005: LBNL group planning meeting to discuss deliverables. A collaboration proposal was submitted to Australia:

November 2005: video conference held between LBNL and CO2CRC collaborators to initiate workscopes. Teams from LBNL and CO2CRC were designated to initiate workscopes in the following areas:

- Flow Simulation
- Geochemical Tracers
- Experimentation /Design UTube
- Seismic Design/Modeling
- Coupled Reservoir Flow/Geomechanical Simulation
- Pressure Transient Analysis

A draft of the collaborative workscope has been completed:

Otway Task 1. Modeling and Simulation
  Task 1.1. Code Comparison (LBNL and CO2CRC)
  Task 1.2. Code Enhancements (LBNL)
  Task 1.3. Investigations of Non-isothermal Effects of CO_2 Injection (LBNL)
  Task 1.4. Modeling Analyses for Site Characterization (LBNL and CO2CRC)
  Task 1.5. Modeling Analyses of Pilot Test (LBNL and CO2CRC)

Otway Task 2. Geochemical Tracers and Fluid/Gas Sampling
        Task 2.1. Enhancement and deployment of the U-tube sampler for application to the Otway Pilot (LBNL and CO2CRC)
        Task 2.2. Install and deploy an on-site mass spectrometer for chemical analysis (LBNL and CO2CRC)
        Task 2.3. Collect baseline geochemical, isotopic and noble gas information on brine and gas samples (LBNL and CO2CRC)
        Task 2.4. Monitor and interpret carbon isotopes in the observation well (LBNL and CO2CRC)
        Task 2.5. Monitor and interpret SF6 and noble gas tracers in the observation well (LBNL and CO2CRC)
        Task 2.6. Use oxygen isotopes to monitor long term exchange of oxygen between CO_2 and H_2O (LBNL and CO2CRC)
        Task 2.7. Analyze and interpret major cation chemistry to evaluate H_2O-CO_2-rock interactions (LBNL and CO2CRC)

Otway Task 3. Active Source Seismic Monitoring
        Task 3.1. Drill a shallow well to deploy a permanent string of seismic sensors (LBNL and CO2CRC)
        Task 3.2. Use a surface seismic source to generate baseline reflections from the reservoir depth at a single location (LBNL and CO2CRC)
        Task 3.3. Repeat the source activation at regular intervals, possibly as a continuous source (LBNL and CO2CRC)
        Task 3.4. Interpret changes in reflected energy as changes in CO_2 saturation (LBNL and CO2CRC)

Otway Task 4. Coupled Reservoir-Geomechanical Fault Stability Analysis
        Task 4.1. Code verification for fault stability analysis (LBNL and CO2CRC)
        Task 4.2. Code enhancement for mechanically induced changes in fault hydrological properties (LBNL and CO2CRC)
        Task 4.3. Pre-injection fault stability assessment of the Pilot Test (LBNL and CO2CRC)
        Task 4.4. Post-test fault stability analysis of the Pilot Test (LBNL and CO2CRC)

Otway Task 5. Pressure Transient Data Collection and Analysis
        Task 5.1. Assemble a hydrologic model and conducting pre-injection pump test predictive calculations (LBNL and CO2CRC)
        Task 5.2. Install downhole and wellhead pressure and temperature gauges in the injection and observation wells (LBNL and CO2CRC)
        Task 5. 3. Pre-injection pump test data collection and interpretation (LBNL and CO2CRC)
        Task 5.4. CO_2 injection and observation well data collection and analysis (LBNL and CO2CRC)

Curt Oldenburg traveled to Barossa, Australia to meet with collaborators of the project. He attended the CO2CRC Annual Technical Meeting, presented a talk on uses of CO_2

injection in depleted gas reservoirs, and discussed impacts of CO_2 injection. A one on one meeting was held to prioritize collaborative modeling tasks and to define a test problem for code inter-comparison studies.

Task 3. Use MMV techniques to evaluate the injectivity and geomechanical response at the In Salah Gas Project in Algeria.

This test provides a unique opportunity to assess the effectiveness of industrial-scale CO_2 storage in a low permeability formation that is representative of many sites in the U.S. The activity will be carried out in cooperation with the In Salah Joint Industry Project (JIP). Since June 2004, the In Salah Gas Project has been injecting nearly one million tonnes per year into the water-filled strata below a depleting gas reservoir. Unlike most CO_2 storage sites, the permeability of the storage formation is low (~ 5 md, less than 1% of the permeability at the Utsira Formation used at the Sleipner Project). In addition, the storage formation, with a thickness of 20 m, is also comparably thin. The small thickness combined with the low permeability results in the need for much higher pressures to inject CO_2. To mitigate high injection pressures, the In Salah Gas Project decided to use long-reach horizontal wells for injection. Participation in this project provides the opportunity to assess the effectiveness of this approach for CO_2 storage in low permeability formations.

The In Salah JIP will carry out detailed monitoring of injection pressures, injection rates, surface fluxes and track subsurface migration of CO_2 using a permanently installed seismic array. The GEO-SEQ activity will complement these planned activities by focusing on the injectivity of this low permeability formation and geomechanical effects due to injection in the unusual long-reach (up to 1.5 km) horizontal wells. Planned activities included obtaining measurements of the distribution of flow along the length of one or more of the horizontal injectors, measuring microseismic activity near the injection wells, obtaining satellite-based interferometry measurements that can assess land surface deformation, and potentially, deployment of tilt meters. These data will be analyzed using coupled flow and geomechanical models (TOUGH2 coupled to a geomechanical simulator). Based on what is learned here, an assessment will be made regarding the feasibility of using long-reach horizontal wells for injection into low permeability formations in other settings, particularly in the U.S.

Task 3 Results and Discussion

Work on this task will begin during the next quarter when funds become available.

Milestones Met

Five abstracts of papers describing the Frio Brine Pilot were presented at the AGU Annual meeting in December 2005. This completes the FY06 QTR1 Milestone. Copies of the abstracts are attached.

Summary of Noteworthy Accomplishments.

- Mapping migration of CO_2 using X-well seismic and Vertical Seismic Profiling (VSP) in a saline formation has been demonstrated for the first time at the Frio Brine Pilot.
- A new method for measuring field-scale relative permeability from pressure transient test data has been developed.
- Five papers describing the Frio Brine Pilot were presented at the AGU Annual meeting in December 2005. This completes the FY06 QTR1 Milestone.

Actual or Anticipated Problems or Delays.

FY2006 funds are needed as soon as possible to assure that the Frio II Pilot test can get underway in the spring of 2006.

Upcoming Events

January 12, 2006. Video-conference regarding the Otway Collaboration

March 20-22, 2006. International Symposium on Site Characterization for CO_2 Storage, Berkeley, CA.

March 14-16, 2006. In Salah SAB Meeting and Workshop, BP Institute, Cambridge, UK.

Seminars and Presentations

October 2005. Second video conference between LBNL and CO2CRC collaborators.

November 2005. CO2CRC Annual Technical Meeting, Barossa, Australia.

December 5-9, 2005. AGU Annual Fall Meeting. San Francisco, CA.

Publications and Abstracts

Benson, S.M., K. Pruess and C.A. Doughty, 2005, Pressure Buildup Data Collection and Analysis During Carbon Dioxide Injection at the Frio Brine Pilot, EOS Trans. AGU, 86(52), Fall Meet. Suppl., December 2005.

Daley, T.M., L.R. Myer, E.L. Majer, J.E. Peterson, 2005, Acquisition of time-lapse, 6-component, P- and S-wave, crosswell seismic survey with orbital vibrator and of time-lapse VSP for CO_2 injection monitoring, 75th annual international meeting of the Society of Exploration Geophysicists, Nov. 2005, Houston Tx.

Daley, T.M., Myer, L., Hoversten, G.M., Peterson, J.E., 2005, Borehole Seismic Monitoring of Injected CO_2 at the Frio Site, EOS Trans. AGU, 86(52), Fall Meet. Suppl., December 2005.

Doughty, C., 2005, Site Characterization for CO_2 Storage and Vice Versa: the Frio Brine Pilot as a Case Study, International Symposium on Site Characterization for CO_2 Geologic Storage, abstract submitted.

Doughty, C., 2005, Glow Modeling for CO_2 Sequestration: The Frio Brine Pilot, EOS Trans. AGU, 86(52), Fall Meet. Suppl., December 2005.

Freifeld, B.M., R.C. Trautz, Y.K. Kharaka, T.J. Phelps, L.R. Myer, S.D. Hovorka and D.J. Collins, 2005, The U-tube: A Novel System for Acquiring Borehole Fluid Samples from a Deep Geologic CO_2 Sequestration Experiment, J. Geophys. Res., 110, B10203, doi: 10.1029/2005JB003735.

Hovorka, S.D., S.M. Benson, C. Doughty, B.M. Freifeld, S. Sakuri, T.M. Daley, Y.K. Kharaka, M.H. Holtz, R.C. Trautz, H. Seay Nance, L.R. Myer and K.K. Knauss, 2005, Measuring Permanence of CO_2 Storage in Saline Formations_the Frio Experiment, Environmental Geosciences Special Issue, submitted.

McCallum, S.D., T.J. Phelps, D.E. Riestenberg, B.M. Freifeld and R.C. Trautz, 2005, Interpretation of Perfluorocarbon Tracer Data Collected During the Frio Carbon Dioxide Sequestration Test, EOS Trans. AGU, 86(52), Fall Meet. Suppl., December 2005.

Trautz, R.C., B.M. Freifeld, C. Doughty, S.M. Benson, T.J. Phelps and S.D. McCallum, 2005, Field Characterization of Reservoir Flow Paths Using Miscible and Immiscible Tracer Tests, EOS Trans. AGU, 86(52), Fall Meet. Suppl., December 2005.